Order Number 1330535

Extraction of surface and subsurface geologic information from digital images of the proposed Arizona Superconducting Super Collider sites

Poulton, Mary Moens, M.S.

The University of Arizona, 1987

U·M·I
300 N. Zeeb Rd.
Ann Arbor, MI 48106

PLEASE NOTE:

In all cases this material has been filmed in the best possible way from the available copy. Problems encountered with this document have been identified here with a check mark __✓__.

1. Glossy photographs or pages __✓__
2. Colored illustrations, paper or print __✓__
3. Photographs with dark background __✓__
4. Illustrations are poor copy _____
5. Pages with black marks, not original copy _____
6. Print shows through as there is text on both sides of page _____
7. Indistinct, broken or small print on several pages __✓__
8. Print exceeds margin requirements _____
9. Tightly bound copy with print lost in spine _____
10. Computer printout pages with indistinct print _____
11. Page(s) _____ lacking when material received, and not available from school or author.
12. Page(s) _____ seem to be missing in numbering only as text follows.
13. Two pages numbered _____. Text follows.
14. Curling and wrinkled pages _____
15. Dissertation contains pages with print at a slant, filmed as received _____
16. Other _____

_____

_____

EXTRACTION OF SURFACE AND SUBSURFACE GEOLOGIC INFORMATION FROM DIGITAL IMAGES OF THE PROPOSED ARIZONA SUPERCONDUCTING SUPER COLLIDER SITES

by

Mary Moens Poulton

A Thesis Submitted to the Faculty of the

DEPARTMENT OF MINING AND GEOLOGICAL ENGINEERING

In Partial Fulfillment of the Requirements
For the Degree of

MASTER OF SCIENCE
WITH A MAJOR IN GEOLOGICAL ENGINEERING

In the Graduate College

THE UNIVERSITY OF ARIZONA

1 9 8 7

STATEMENT BY AUTHOR

This thesis has been submitted in partial fulfillment of requirements for an advanced degree at the University of Arizona and is deposited in the University Library to be made available to borrowers under rules of the Library.

Brief quotations from this thesis are allowable without special permission, provided that accurate acknowledgment of source is made. Requests for permission for extended quotation from or reproduction of this manuscript in whole or in part may be granted by the head of the major department or the Dean of the Graduate College when in his or her judgment the proposed use of the material is in the interests of scholarship. In all other instances, however, permission must be obtained from the author.

SIGNED: Mary Maus Paul

APPROVAL BY THESIS DIRECTOR

This thesis has been approved on the date shown below:

Charles E. Glass
Professor of Geological Engineering

4/22/87
Date

ACKNOWLEDGMENTS

I want to express my gratitude to the many people who helped me see this project through to the end. I would like to thank Drs. Charles E. Glass and Ben K. Sternberg for their help in editing my thesis and serving on my committee. A very special thanks to Dr. John L. Thames who was both gracious and generous with the help he provided.

In addition, I wish to thank Dr. Albert Weaver for providing the funding for the image processing work and Dr. Robert Schowengerdt for his technical guidance.

Finally, I wish to thank my husband William. It was his unselfish support, encouragement and patience that made the long days and late nights of work possible throughout my graduate studies.

TABLE OF CONTENTS

LIST OF TABLES

LIST OF ILLUSTRATIONS

LIST OF ILLUSTRATIONS—Continued

ABSTRACT

Digital image processing techniques and analyses were conducted on Landsat MSS and digital elevation data as part of the Arizona site investigation for the Superconducting Super Collider.

Analysis of MSS band 7/band 5 ratio images indicated a high-density riparian community on the southeast flank of the Sierrita Mountains. Runoff was calculated using the U.S. Soil Conservation Service runoff model and a water budget. The results indicate that many of the sectors around the Sierrita site could support similar stands of vegetation. Subsurface geology is probably the most significant factor in the localized occurrence of the dense vegetation.

A MSS band 7/band 5 ratio image was calculated for the Maricopa site. The occurrence of the dense vegetation was correlated with the location of clay-filled basins on the east side of the Maricopa Mountains. Mountain-pediment-bajada contacts were delineated using a density slice of an MSS band 7 image and a slope magnitude image.

CHAPTER 1

INTRODUCTION

The Superconducting Super Collider (SSC) is a 20 trillion electron-volt (20 TeV) proton synchrotron under consideration by the U.S. Department of Energy for experiments in high-energy physics. Several states, including Arizona, are preparing proposals to attract the SSC. Qualified proposals will be reviewed by a panel of distinguished individuals appointed by the Presidents of the National Academy of Sciences and the National Academy of Engineering. This panel will select the most outstanding proposals for detailed consideration by the Department of Energy, which will make the final decision (University Research Association 1985, p. 27). Two sites are being investigated in Arizona for SSC consideration, one around the Sierrita Mountains south of Tucson and one in the Maricopa Mountains west of Phoenix. Reports on both sites will be submitted to the State and one site will be selected for submission to the SSC review panel.

The most impressive aspect of the SSC is its size. Current design criteria call for a planar ring (a combination of short, straight sections and arcs approximating a circle) with a circumference of 51.5 miles, a tunnel diameter of 10 feet and a minimum depth of burial of 20 feet. At six regions around the ring, the countercirculating proton beams will collide and experiments will be conducted. A campus-type facility will be adjacent to the ring to

provide office space for the staff. The site must be large enough to accommodate the accelerator with possibility of a slight tilt (<1 degree) to accommodate the profile of the ring and topography. Approximately 11,000 acres of land distributed around the ring will be required.

Vegetation density was examined at both the Sierrita and Maricopa sites using MSS band 7/band 5 ratio images. A high-density riparian community was revealed on the southeast flank of the Sierrita Mountains. Runoff was calculated for the site using the Department of Watershed Management's computer program MULT. The Soil Conservation Service (SCS) runoff equation is used in MULT. A water budget was also calculated showing the distribution of precipitation between runoff and losses. The evapotranspiration of the vegetation was estimated based on densities estimated from the ratio image. The runoff and evapotranspiration data were used to help explain the localized occurrence of dense riparian vegetation in the southeast section of the proposed SSC.

At the Maricopa site, clay has accumulated in basins on the east side of the Maricopa Mountains. Because the clay may pose construction problems, the areal extent of the basins that contain it should be defined. Mountain-pediment-basin boundaries were delineated based on information from a vegetation density image, an MSS near-infrared image, and a slope magnitude image.

CHAPTER 2

DESCRIPTION OF IMAGERY

A digital image is any image composed of discrete elements called pixels whose values are determined by a measurement of some physical property. In the case of Landsat MSS imagery, the brightness value for each pixel is derived from a measure of the amount of radiation reflected in discrete spectral bands from a 79 x 79 meter ground resolution cell. A Landsat MSS scene covers approximately a 185 x 185 kilometer area. The spectral range of the MSS bands is listed in Table 1. A description of the computer computible tapes (CCTs) used for this thesis is listed in Table 2.

The image used for the Sierrita site was extracted from a preprocessed Landsat CCT. Preprocessing restores the aspect ratio of the scene. The November vegetation density images for the Sierrita site were extracted from unpreprocessed Landsat CCTs. The image used for the Maricopa site was also extracted from an unpreprocessed CCT and spatially registered to the Maricopa County digital elevation data. All of the Landsat imagery used was acquired from the Department of Mining and Geological Engineering's Digital Image Library.

The U.S. Defense Mapping Agency (DMA) has digitized 200-foot elevation contours from all 1:250,000 AMS series maps of the contiguous United States. The Arizona State Land Department has acquired these digital terrain data for the entire State of Arizona. The State

TABLE 1

SPECTRAL RANGE OF MSS BANDS

BAND	WAVELENGTH (nm)
4	500 - 600
5	600 - 700
6	700 - 800
7	900 - 1100

TABLE 2

DESCRIPTION OF IMAGERY

Site	Scene/ Frame ID	Date	Solar Elevation	Solar Azimuth
Maricopa	21234-17044	6/9/78	56	97
Maricopa	2873-17010	6/13/78	56	97
Sierrita	2296-17143	11/14/75	33	135
Sierrita	20494-17101	5/30/76	59	100

Land Department resampled the data to a nominal pixel size of 77 meters for Maricopa County. The elevations were coded into 8-bits (256 gray levels). Each gray level represents 9 meters of relief for the Maricopa County data. Tables to convert gray levels to elevations were provided with the data set. These data are no more accurate than the contour maps from which they were derived. Unknown errors may exist from the numerous interpolations that were performed. Artifacts exist in the data set where two AMS sheets were merged when digitizing.

All image processing for this thesis was performed at the Digital Image Analysis Lab (DIAL) at the University of Arizona using Model S570 software from International Imaging Systems (I^2S) and System at Arizona for Digital Image Experimentation (SADIE) software on a Vax 11/750.

CHAPTER 3

DESCRIPTION OF SITES

Several sites around the state were initially considered for the SSC. Concerns about proximity to major airports, geology, land ownership and subsidence helped narrow the choices to two, the Sierrita site and the Maricopa site.

Sierrita Site

A contrast-enhanced Landsat MSS false-color composite of the Tucson area shows the Sierrita Mountains and surrounding pediment (Figure 1). The Sierrita site for the SSC encircles the Sierrita Mountains 20 miles southwest of Tucson, Arizona. The site is bounded by the San Xavier Indian Reservation on the north, a large porphyry copper mining district to the east, the Cerro Colorado Mountains and Bob White Refuge to the south and Altar Wash to the west. The site is dominated by Laramide age Ruby Star Granodiorite uplifted to form the Sierrita Mountains. The highest point is Red Boy Peak at 6,000 feet. The main mountain mass is surrounded by a broad pediment which begins at about 4,500 feet at the base of the mountain and slopes gradually to 3,000 feet at Altar Wash and the Santa Cruz River. Several isolated peaks rise more than 500 feet above the pediment. The alluvial slopes on the southeast flank are dissected by numerous ephemeral streams. Drainages are very sparse on the north flank. The arcuate

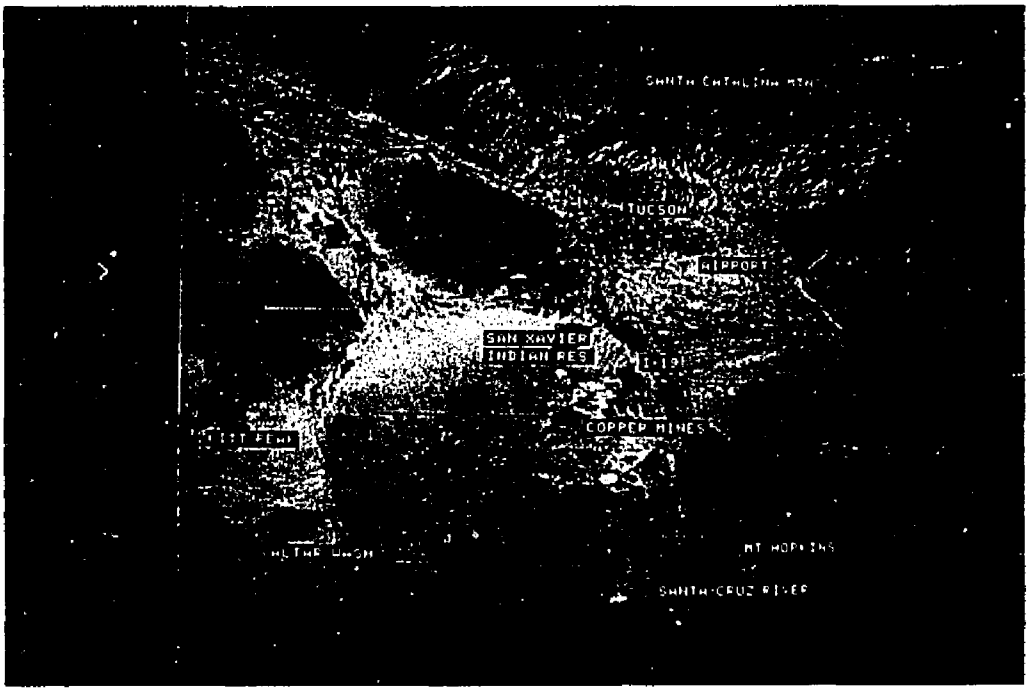

Figure 1. Tucson Landsat MSS Scene

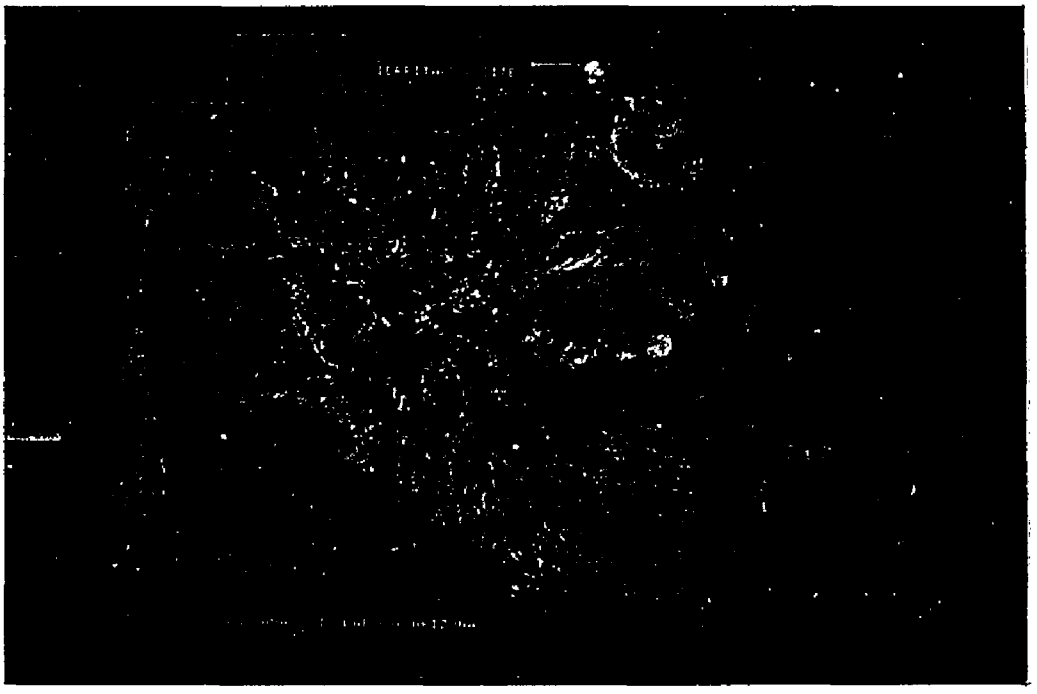

Figure 2. Sierrita Landsat MSS Scene

boundary north of the Sierrita Mountains marks the pediment-basin boundary. Altar Wash is the major drainage to the west. The Santa Cruz River is the major drainage to the east.

Figure 2 shows the Sierrita site in more detail. This image shows the major drainages and the change in drainage density from the north flank of the Sierritas to the south. The greater drainage density and vegetation cover on the southeast flank are believed to be due to the orographic effect. This is the effect of mountain uplift on air mass movement. At the Sierrita site, it concentrates the precipitation on the southeast flank. The Tertiary Tinaja Peak andesite and rhyolite flows are visible on the east flank south of the mines. Tertiary volcanics and sediments of the Cerro Colorado Mountains are visible south of the Sierrita Mountains. The greenish-yellow areas associated with drainages in the south and southeast are dark red Pleistocene clay horizons. These horizons are usually overlain by a layer of permeable sand and gravel, but in some areas the overlying horizon is very thin or has been eroded. The volcanic Black Hills are visible on the southwest flank. A northwest trending Precambrian, Paleozoic and Mesozoic wedge of phyllitic rhyolite, dolomitized limestone and massive quartzites is clearly visible on the west flank of the Sierrita Mountains.

Red in the image corresponds to vegetation. Much of the vegetation, predominantly juniper, in the mountains is concentrated on the cooler north slopes. The stream channels on the southeast side are heavily vegetated with mesquite. Many of the faults cutting through

the Precambrian-Mesozoic strike belt are visible because of vegetation growing in these more permeable zones.

The Pantano, Tinaja and Ft. Lowell Formations are the alluvial units surrounding the Sierrita Mountains. They are part of the aquifer system in the Tucson Basin. The Ft. Lowell Formation provides most of the groundwater withdrawn in the Sierrita area (Davidson 1973). The depth to the water table is not known precisely but is believed to range from 50 to 300 feet on the east side of the site and 300 to 400 feet on the west side (Davis and Brooks 1986).

Maricopa Site

The Maricopa site for the SSC is in the Maricopa Mountains 30 miles southwest of Phoenix, Arizona (Figure 3). The site is bounded by the Little Rainbow Valley to the east, Interstate 8 to the south, State Route 85 to the west and the Gila River to the north. The site lies within a Bureau of Land Management Wilderness Area.

Figure 4 shows the Maricopa site in more detail. The site is dominated by 1.4 billion-year-old Precambrian granite that has been undergoing erosion for the past 4 million years (Krason et al 1982). The mountains are steep and have a relief of about 2000 feet. The highest point is at 2800 feet. The elevation of the surrounding pediment ranges from 800 to 1400 feet. Fault scarps have been eroded back considerable distances to form extensive pediments and the range fronts are deeply embayed. There is a pronounced north-south to northwest trending topographic grain which reflects the Miocene Basin and Range normal faulting.

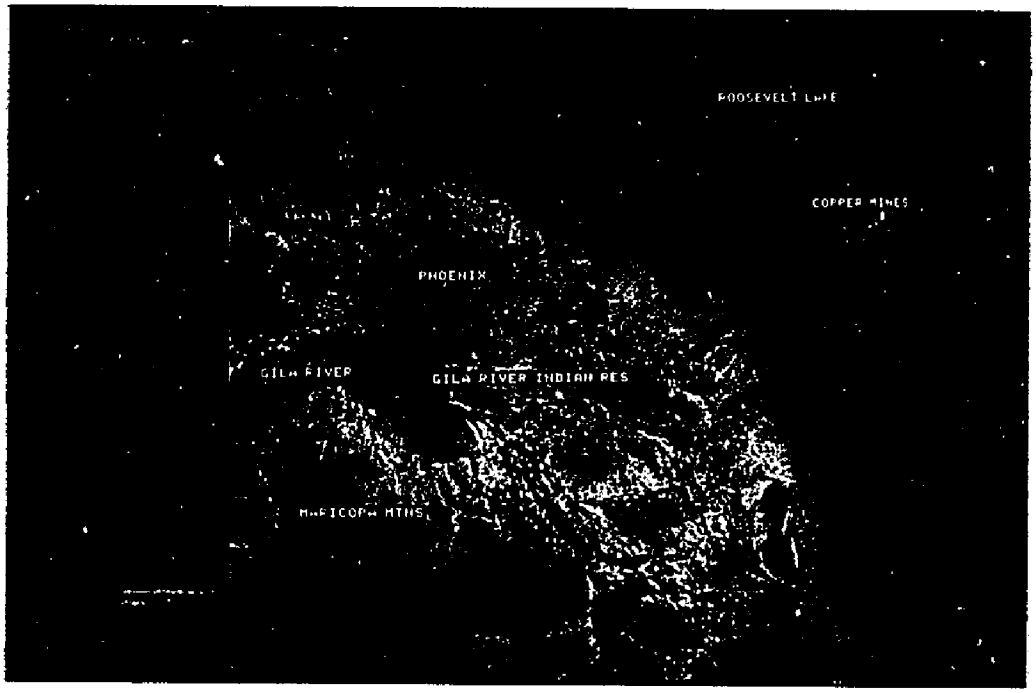

Figure 3. Phoenix Landsat MSS Scene

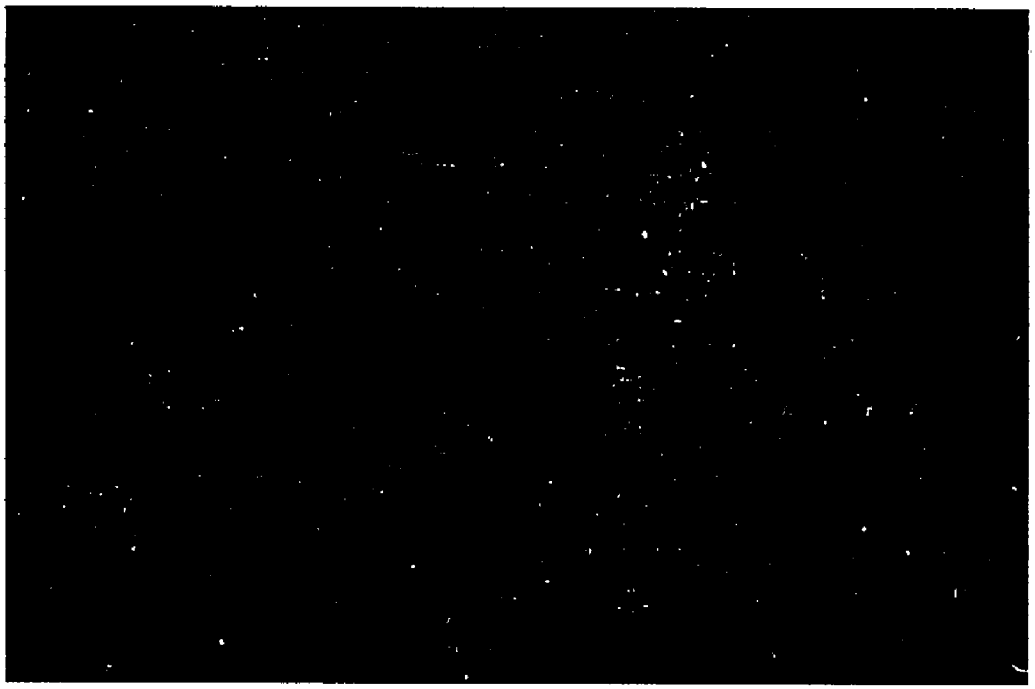

Figure 4. Maricopa Landsat MSS Scene

The lithology is more homogeneous than at the Sierrita site. Precambrian granite with some mylonitic, schistose and pegmatitic textures is the dominant rock unit. Some Precambrian roof-pendant schist is found in the south central Maricopa Mountains. The Maricopa Mountains have not been mapped or studied in great detail to date. Few details are known about lithology, alluvial units, fracture sets or depth to groundwater.

Agricultural cultivation and irrigation occur in the Little Rainbow Valley to the east and Mobile Valley to the southeast. The Gila River is the major drainage to the north and west. Waterman Wash is the drainage to the east.

CHAPTER 4

ANALYSIS OF VEGETATION DENSITY AT THE SIERRITA SITE

A vegetation density image of the Sierrita site revealed a unique high-density riparian community on the southeast flank of the Sierrita Mountains. Since no other area at the Sierrita site supports such dense vegetation, an explanation for its occurrence is sought through analysis of a water budget at the site. Runoff was calculated using the Department of Watershed Management's computer program MULT. The distribution of precipitation between runoff and losses was estimated using a water budget from the Walnut Gulch Experimental Watershed. Evapotranspiration was estimated from the vegetation density. All these data were used to determine if the dense vegetation was a result of a unique hydrologic regime.

The watersheds in the Sierrita Mountains are not gauged, so no site-specific data on runoff and precipitation exists. The U.S. Soil Conservation Service (SCS) developed a method to calculate direct runoff in ungauged watersheds which requires knowledge of precipitation, soil type and land use or vegetation cover. In addition, MULT requires information on the effective hydraulic conductivity of the stream channels. Site-specific data on soil type and vegetation cover in the form of Landsat images and an SCS soil survey exist for the Sierrita Mountains. Annual precipitation data were extrapolated from stations in the vicinity. Daily precipitation data were obtained from

MULT. Information on effective hydraulic conductivities was obtained from Lane (1983, p. 19.5).

Runoff Model

The derivation of the SCS runoff equation begins with the relationship between runoff and retention of precipitation disregarding any initial abstraction of precipitation (SCS 1972, p. 10.3). Initial abstractions of precipitation include interception by the vegetation canopy, infiltration and surface storage.

$$F/S^1 = Q/P, \quad (1)$$

where F = actual retention,

S^1 = potential maximum retention,

Q = actual runoff,

P = potential maximum runoff

$$\text{and } F = P - Q, \quad (2)$$

$$\text{hence } (P - Q)/S^1 = Q/P \quad (3)$$

$$\text{and } Q = P^2/(P + S^1). \quad (4)$$

If the initial abstraction (Ia) is included in the calculations, then equation (1) is modified as follows:

$$F/S = Q/(P - Ia) \quad (5)$$

$$S = S^1 + Ia$$

$$F = (P - Ia) - Q \quad (6)$$

From experimental watersheds

$$Ia = 0.20 * S, \quad (7)$$

$$Q = (P - 0.20 * S) / (P + 0.80 * S) \quad (8)$$

$$\text{and } S = (1000/CN) - 10. \quad (9)$$

CN is a hydrologic soil-cover complex number also known as a curve number. The soil type is matched to a soil group in Table 3. The soil group is cross-matched with the cover classification in Table 4 to find the curve number. The retention S is calculated and substituted into equation (8) along with a precipitation value to find the runoff.

Precipitation

The first parameter required by the SCS runoff equation is precipitation. Daily precipitation records were accessed in the program MULT by latitude, longitude and elevation of the area of interest. A Monte Carlo simulation was used to vary the magnitude of the precipitation events and the interarrival time between events (Henkel 1985). Thirty years and five different interarrival sequences were simulated for each sector.

Annual climate data from eight stations in the vicinity of the Sierrita Mountains (Table 5) were gathered and analyzed by Zauderer (1986a). The period of record for these stations was 41 years, 1931 to 1972. A linear regression between precipitation and elevation was found to fit best for five of the stations (Figure 5). An isohyetal map was produced for the Sierrita Mountains (Figure 6) based on station record and elevation-precipitation relations for those five stations in addition to vegetation and Landsat multi-temporal images of bands 5 and 7 and a 7/5 band ratio (Zauderer 1986a, p. 13).

TABLE 3

SUMMARY OF HYDROLOGIC SOIL GROUPS AND THEIR CHARACTERISTICS USED TO DEFINE RUNOFF CURVE NUMBERS (CN)

(Lane 1984)

Soil Group	Typical or Unusual Characteristics	Comments
A	High infiltration rates even when wetted. Well-drained to very well drained gravel, sand, loamy sands and sandy loams. Soils with depths of 36 in. or more without infiltration reducing or restricting layers.	Low runoff potential and very low CNs. Final infiltration rates on the order of 0.3 to 0.4 in/h or higher.
B	Moderate infiltration rates. Moderately well-drained to well-drained soils with moderately fine to somewhat coarse texture. Usually soils with depths of 20 in. or more.	Low to moderate runoff potential and CNs. Final infiltration rates on the order of 0.16 to 0.3 in/h.
C	Slow infiltration rates. Moderately fine to fine texture or infiltration reduction caused by layering. Usually 20 in. or less of soil over an infiltration reducing layer.	Moderate to high runoff potential and CNs. Final infiltration rate on the order of 0.04 to 0.16 in/h.
D	Very slow infiltration rates. Clay soils with swelling potential. Shallow soils over nearly impervious material. Usually less than 12 in. of soil over a layer restricting infiltration.	High runoff potential and CNs. Final infiltration rate of 0.04 in/h or less.

TABLE 4

RUNOFF CURVE NUMBERS FOR VARIOUS HYDROLOGIC SOIL GROUP-COVER COMPLEXES, ANTECEDENT MOISTURE CONDITION II

(Lane 1984)

	Runoff Curve Numbers By Soil Groups			
Cover Type and Conditions	A	B	C	D
Hard, compacted surfaces such as dirt roads, etc.	74	84	90	92
Unimproved bare soil	72	82	87	90
Desert brush				
10% cover	-	84	88	93
20% cover	-	83	87	92
40% cover	-	82	86	90
Pasture or range				
poor	68	79	86	89
fair	49	69	79	84
good	39	61	74	80
Herbaceous plants, brush, and grass				
20% cover	-	79	86	92
40% cover	-	74	82	90
Pinon/juniper/grass				
40% cover	-	65	75	88
60% cover	-	57	70	86
80% cover	-	48	62	83
Ponderosa pine				
40% cover	-	61	75	80
60% cover	-	55	70	77
80% cover	-	49	65	73

TABLE 5

LOCATION OF PRECIPITATION STATIONS

Name of Station	Latitude Longitude	Altitude
Sahuarita	31°58', 110°58'	2690 (ft.)
Anvil Ranch	31°59', 111°23'	2750
Amado	31°42', 111°04'	3100
Helmet Peak	31°57', 111°03'	3220
Ruby Star Ranch	31°55', 111°05'	3640
Arivaca 1E	31°35', 111°19'	3675
Fresnel Ranch School	31°49', 111°32'	3700
Santa Margarita	31°91', 111°35'	3925

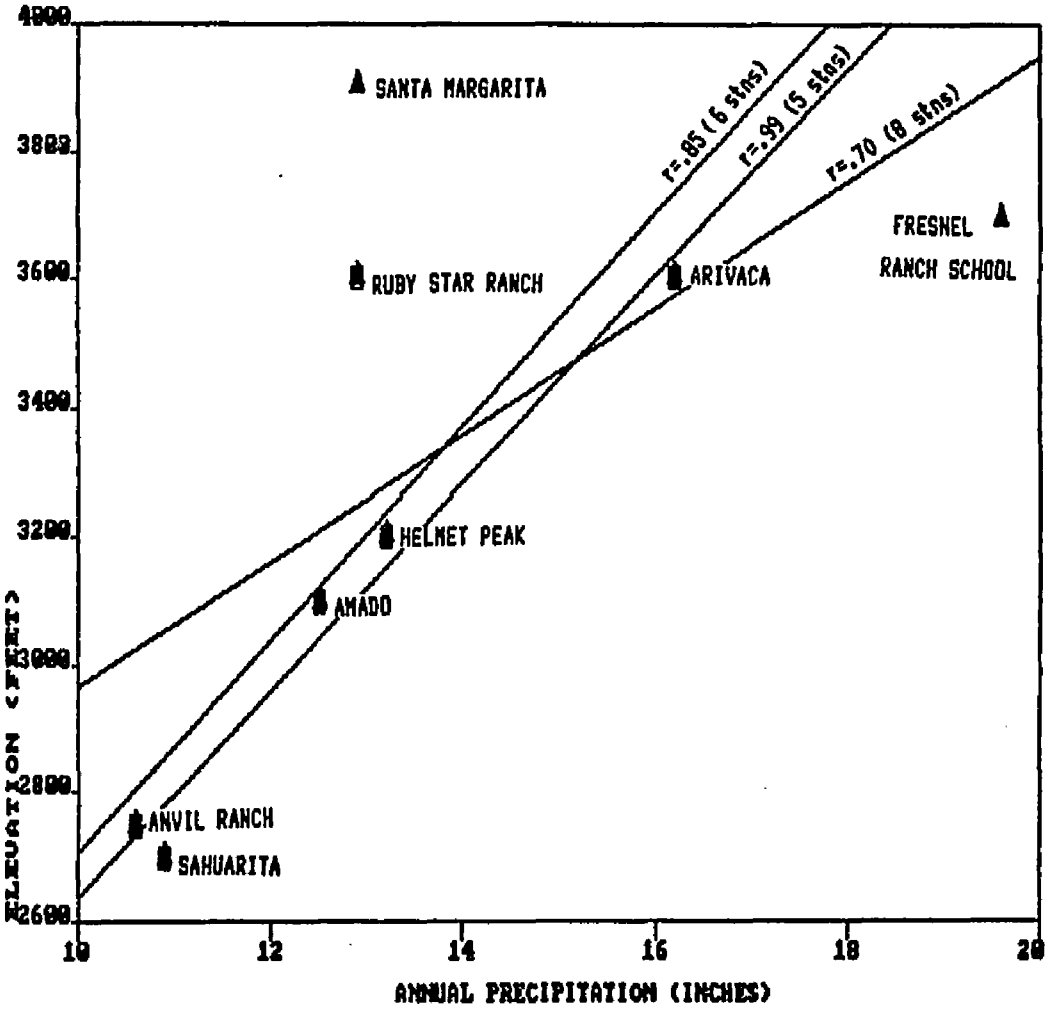

Figure 5. Correlations of Average Annual Precipitation to Elevation: 8, 6 and 5 Stations (Zauderer 1986a)

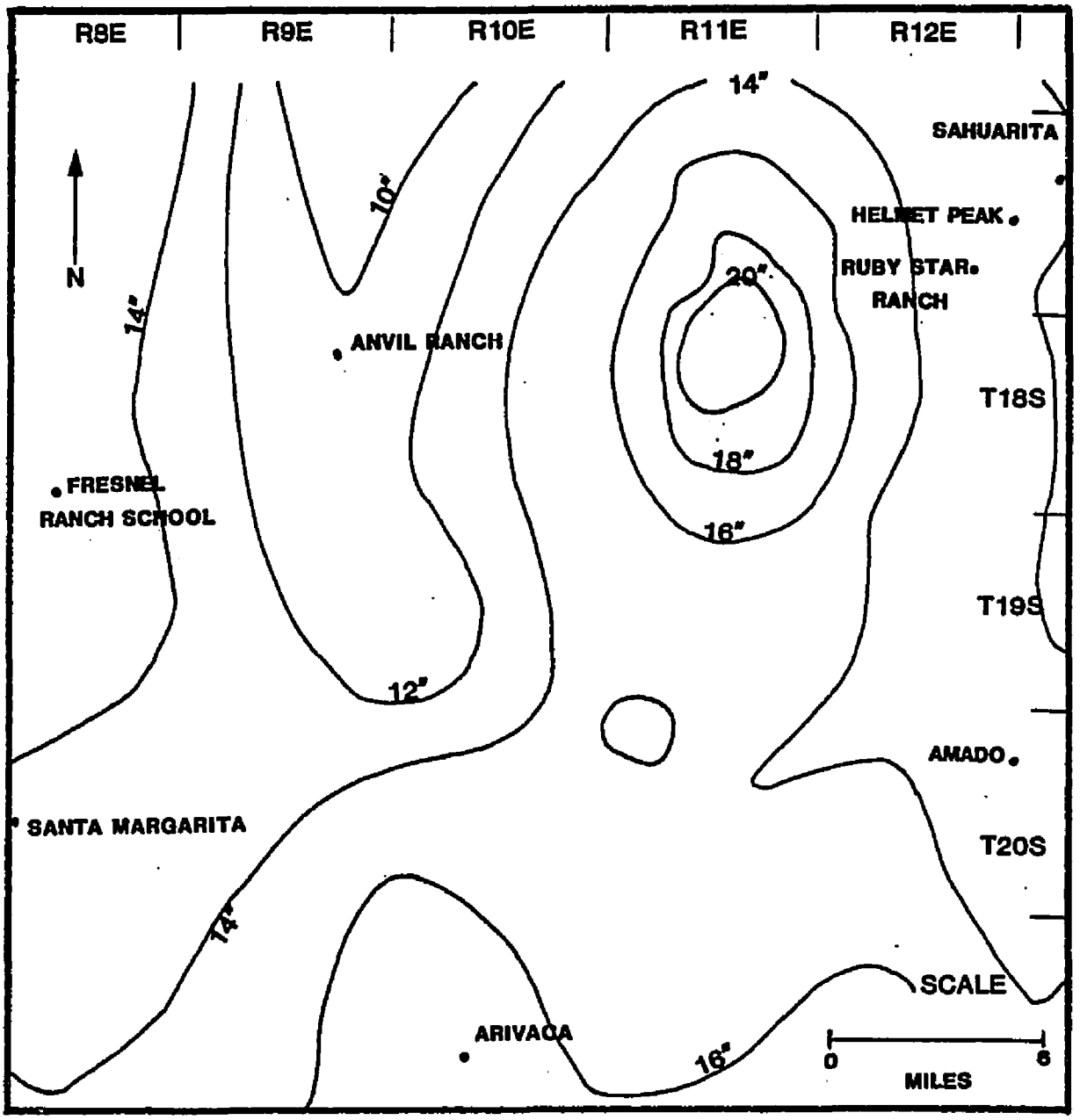

Figure 6. Isohyetal Map of Sierrita SSC Site (Zauderer 1986a)

Soils

The U.S. Soil Conservation Service completed a soil survey for Pima County which included the Sierrita Mountains (SCS 1986). Data that related to the SSC location were extracted by Zauderer (1986b). Specific soil types vary widely in any given location around the Sierrita Mountains, so where necessary the soil type with the largest areal extent or dominant runoff characteristic was included in the selection of a soil group. Soil profiles on the northern flank consist of coarse horizons of sandy loam overlying shallow bedrock. Soil profiles on the southern flank generally consist of an upper 2-foot clayey-loamy horizon and a well-developed clay horizon beneath. The clayey-loamy horizon accumulates very slowly with years of vegetation cover. It is easily eroded in places where the vegetation has been stripped.

A Landsat MSS band 4/band 5 ratio was calculated for the site (Figure 7). This ratio image enhances surface exposures of a dark red clay horizon. This clay horizon, the White House-Caralampi Complex or Sasabe-Caralampi Complex, has a medium to high runoff potential. It dominates the soil characteristics for soil group classification in the subsectors where it is present. An exposure of this horizon is shown in Figure 8. The clay horizon is overlain by an inch of clay loam and a surface coating of gravel and pebbles. The horizon is underlain in places by a highly impervious tuffaceous conglomerate. The tuffaceous conglomerate weathers to a very gravelly fine sandy loam along the stream channels on the southeast flank of the Sierrita Mountains (Zauderer 1986, p. 44).

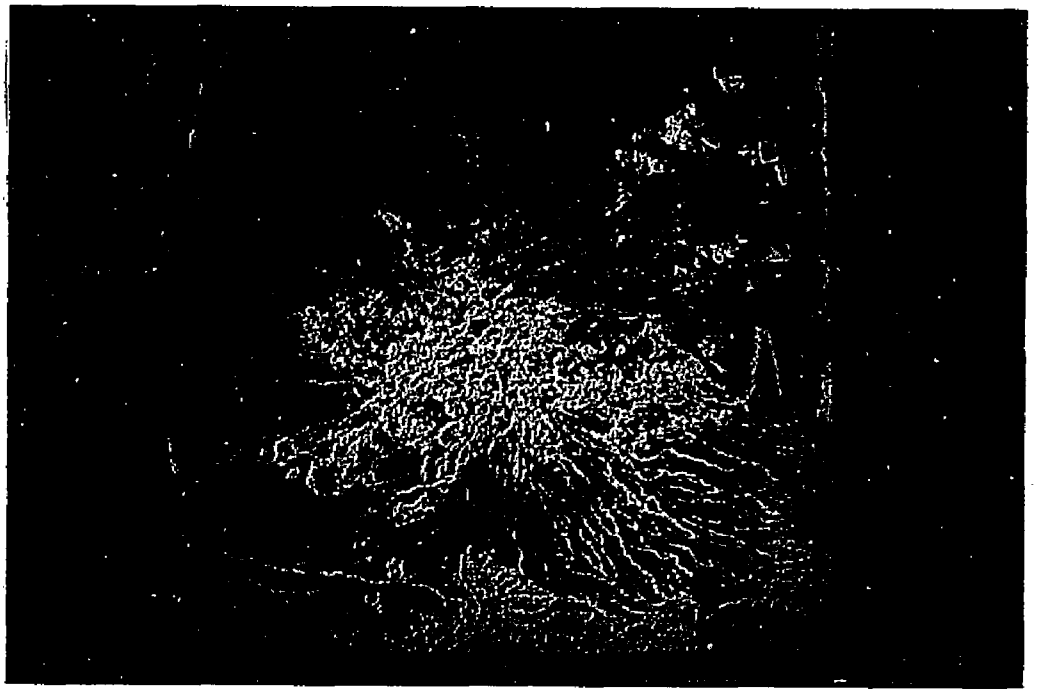

Figure 7. Landsat MSS Band 4/Band 5 Ratio.
Red represents surface exposures of red clay.

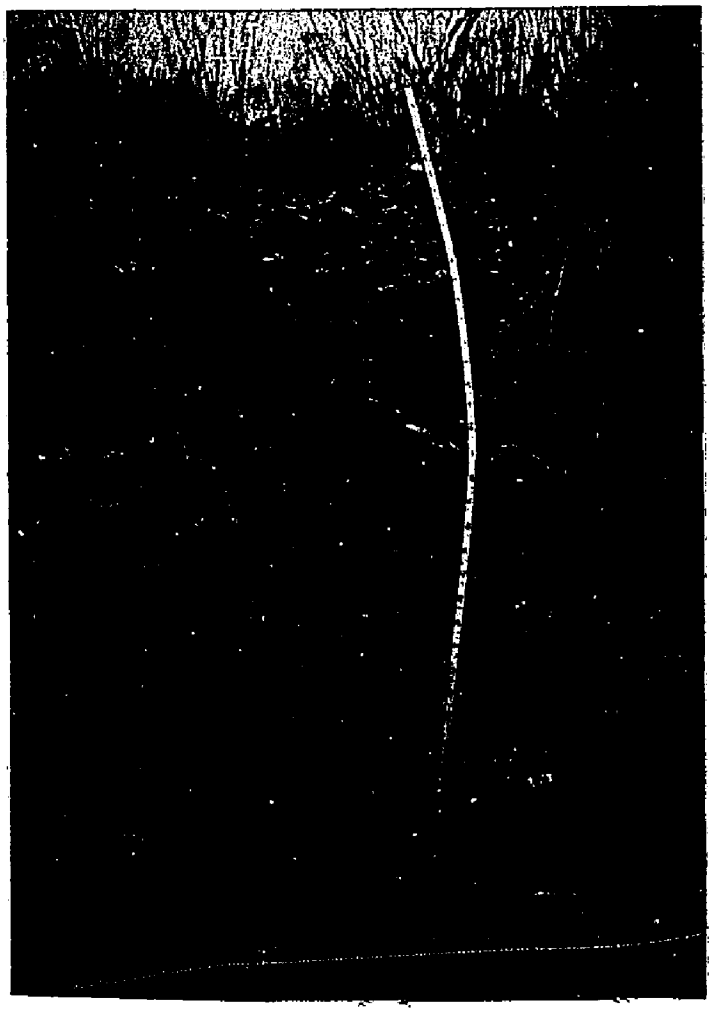

Figure 8. Soil Cut Exposing Red Clay Horizon

Vegetation Cover

The efficacy of Landsat MSS data for analyzing land use and vegetation density is well documented (Rango, Foster and Salomonson 1975; Ragan and Jackson 1975). The density and areal extent of the vegetation had to be ascertained for evapotranspiration estimates and for determination of curve numbers. Multi-temporal images from November 1975 and May 1976 were used in this analysis to assess the seasonal variation of the vegetation density.

Vegetation Reflectance Model. The absorption, reflection and transmission of a vegetation canopy is due to the chemical and physical properties of its leaves (Knipling 1970, p. 155; Gates et al 1965, p. 12) (Figure 9). Chlorophyll pigments are the main absorbers of radiation in the visible portion of the spectrum. As much as 50% of the energy in this region that strikes a leaf is absorbed. There is a slight peak in the reflectance at 550 nm, which accounts for the green color of vegetation. Chlorophylls are completely transparent to infrared radiation; hence the high reflectance between 680 and 1200 nm is due to the large number of air-cell wall interfaces in the mesophyll. Beyond 1400 nm, the reflectance is attributed to the water content of the leaf. Thus, the reflectance spectra for vegetation represents a dynamic response to its radiant environment.

Quantifying Vegetation Density. Some four dozen formulae have been developed to qualitatively and quantitatively assess the vegetation canopy (Perry and Lautenschlager 1984, p. 169). Most formulae are based on ratios or linear combinations and exploit differences in the reflectance patterns of green vegetation. The simplest vegetation

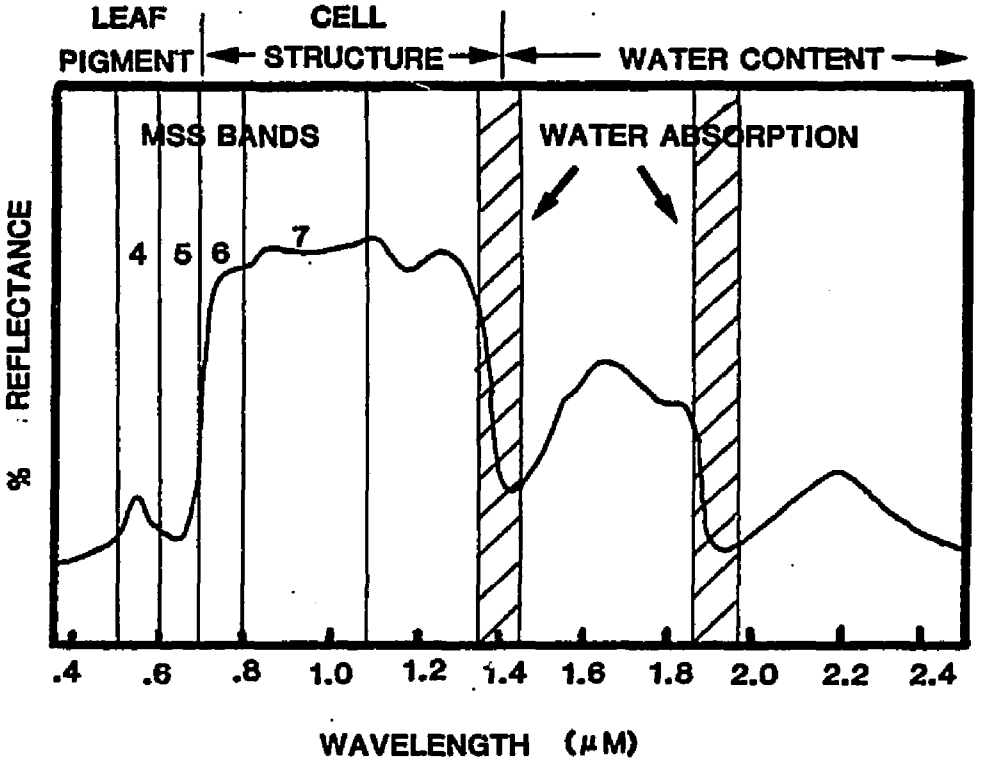

Figure 9. Generalized Vegetation Reflectance
(Goetz et al 1983)

indices that assess percent ground cover and biomass are the ratios MSS band 7/band 5 (R75), MSS band 6/band 5 (R65), bands 7-5/bands 7+5 (normalized difference ND75), bands 6-5/bands 6+5 (normalized difference ND65) and the transformed vegetation indices (TVI) $(ND75 + 0.5)^{1/2}$ or $(ND65 + 0.5)^{1/2}$. All of these indices show an approximate linear relationship to biomass or percent cover (Raines et al 1978, Curran 1980, Perry and Lautenschlager 1984), depending on the type of vegetation considered. More elaborate equations such as the Kauth-Thomas "Tasselled Cap Transformation" (Kauth and Thomas 1976) or the perpendicular vegetation index rely on linear transformations of the data to separate vegetation from soil spectra.

The normalized differences and transformed vegetation indices are functionally equivalent for decision making to the basic ratios R65 and R75. That is, decisions made on the basis of one index could have been made equally well on the basis of the other index. The value of one index can be computed from the value of the other index. Perry and Lautenschlager (1984, p. 171) state that the use of the more complicated indices can only be justified if they improve the regression fit or normalize the regression errors when correlating field measurements with digital counts in the image.

Raines et al (1978) found that R65 correlated better to percent cover for rangeland than R75. Curran (1980) and Tucker (1979) have found R75 to be a more accurate index for most vegetation. Rouse et al (1973) found TVI65 was more sensitive to biomass estimates. Both R65 and R75 were computed for the Sierrita site. Even though bands 6 and 7 are highly correlated, the vegetation densities

calculated were different. The R75 showed more subtle changes in high density areas.

A ratio of band 7 divided by band 5 was selected for this study. A correction was made to band 5 to compensate for atmospheric scattering. A dark object subtraction method was used. The near-infrared band, band 7, should have some pixels with a gray level near zero if water bodies or shadows are present. Presumably the other bands will also have some gray levels near zero. The dark object subtraction method involves shifting the histograms of each band so that the minimum gray level is near zero. Band 7 needed no correction in the images used, but band 5 did. The minimum gray level of band 5 was subtracted from the mean so that the resulting minimum gray level was near zero.

The R75 vegetation densities were classified by pseudocoloring the May and November images (Figure 10). Pseudocoloring assigns a color scale to the gray levels in the image. The number of gray levels assigned to each color can be controlled interactively by adjusting the cursor position in the S570 program PSEUDO'COLOR. A color scale was added to the image to calibrate the pseudocolor coding.

In the absence of field data, the vegetation density was assumed to be linearly related to the gray levels in the ratio image. When the image was pseudocolored, the color assigned to the copper mines was equated to 0% cover and the color assigned to the agricultural fields was equated to 100% cover. The intermediate colors were linearly scaled between these two limits.

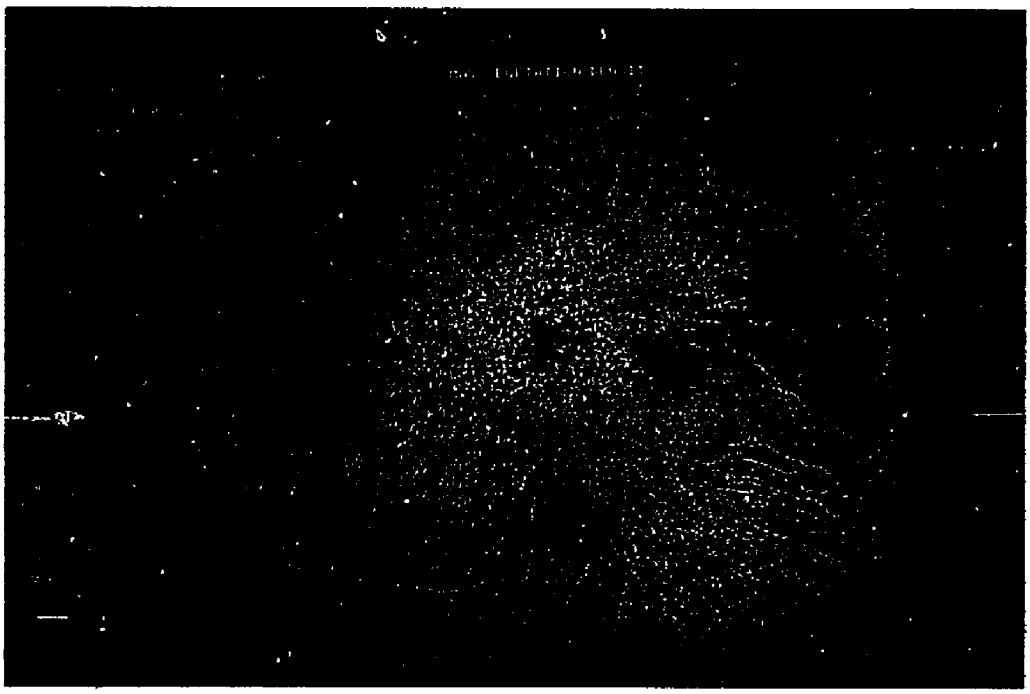

Figure 10a. May Vegetation Density for Sierrita Site

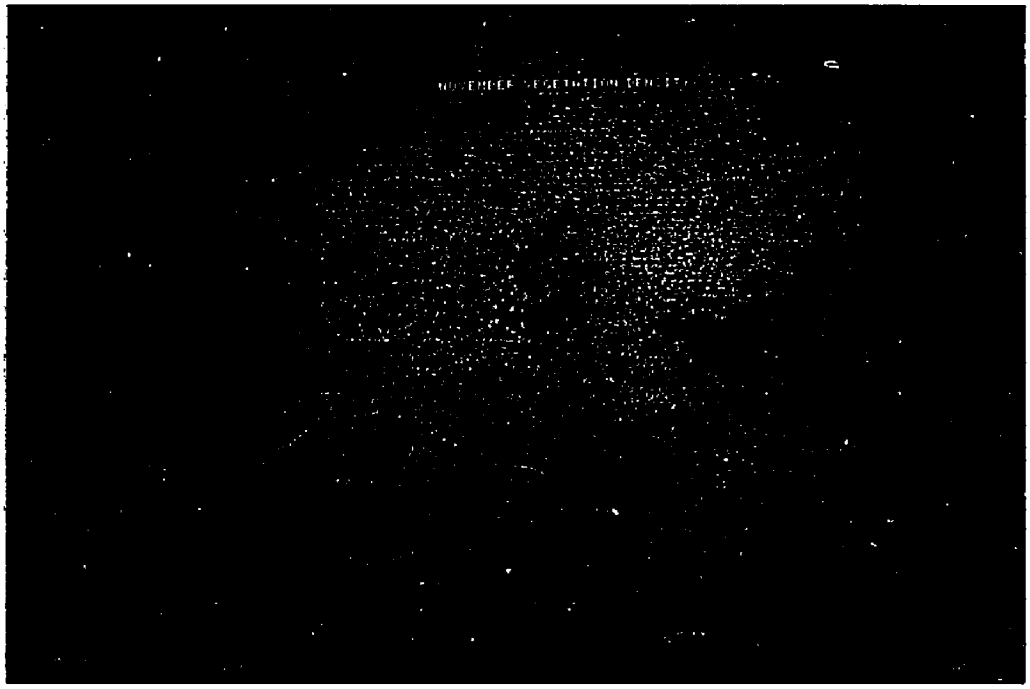

Figure 10b. November Vegetation Density for Sierrita Site

The May vegetation density image more clearly defines the riparian vegetation. The riparian trees are in full leaf by May, but the surrounding brush is not growing as vigorously. In November, the riparian trees are senescencing while the surrounding brush is growing more vigorously. The May image was used to define areas of greatest consumptive use. The areal extent of the 80-100% class (black color in Figure 10) and 60-80% class (yellow color in Figure 10) were calculated from histograms of each sector for the May image.

Selection of Curve Numbers

The Sierrita site was divided into eight sectors (Figure 11) based on major drainage divides, drainage density and soil types. Each sector was divided into subsectors with uniform precipitation. Each sector ended at a major wash or river except on the north side of the mountains. Those sectors were terminated at the boundary between T15S and T16S, since there are no major drainages on the north side and the data for annual precipitation and vegetation density ended there. A curve number was selected for each subsector based on the dominant soil type and vegetation cover. Curve numbers and areas for each subsector are listed in the Appendix.

Transmission Losses

Transmission losses are losses due to infiltration into the bed, banks and flood plain of a stream channel. These losses significantly reduce the runoff in arid and semiarid regions. Transmission losses are the primary groundwater recharge source in limited rainfall areas (Renard 1970, p. 19). The program MULT requires information on

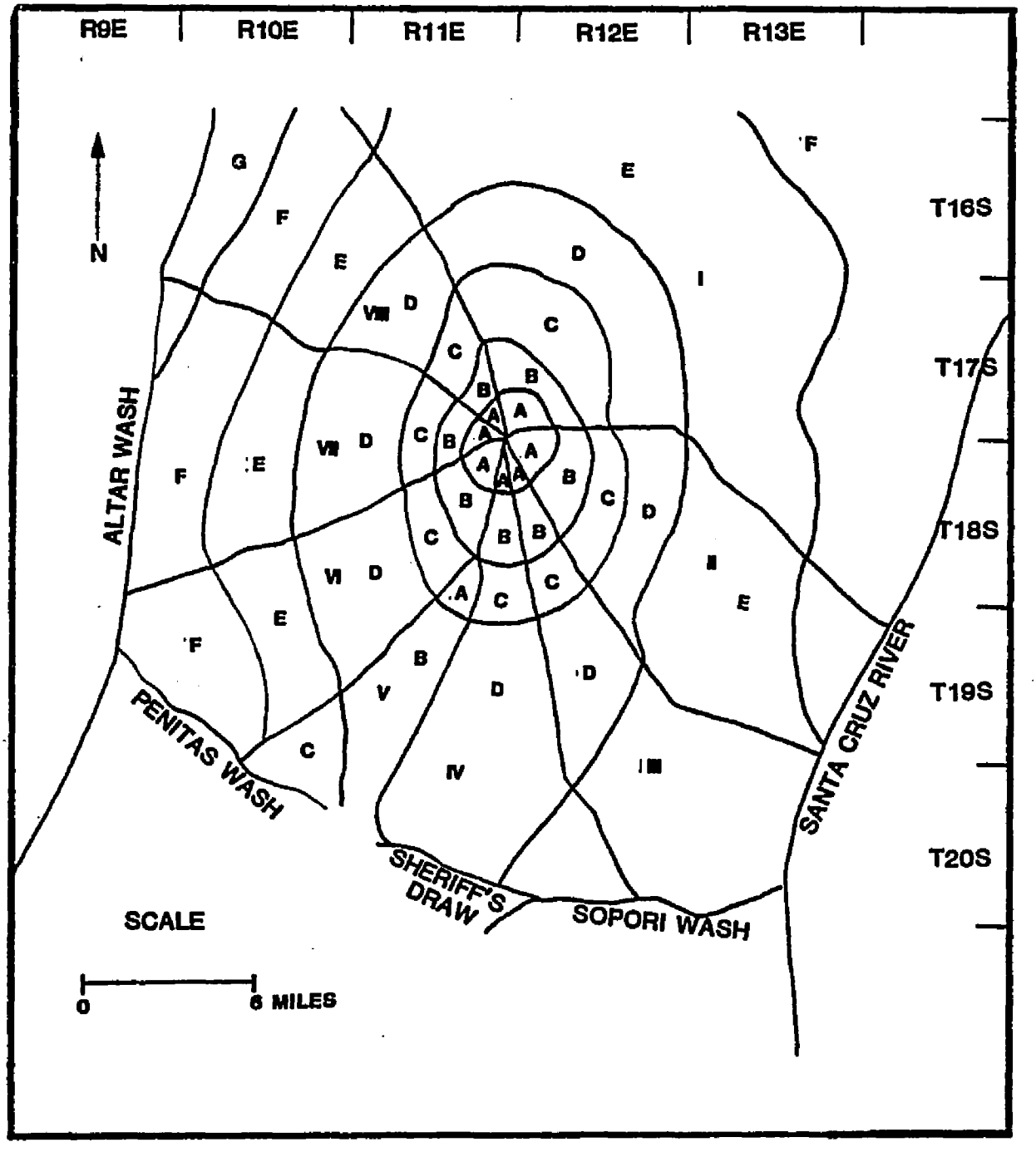

Figure 11. Map Showing Location of Subsectors for Sierrita Site

TABLE 6

RELATIONSHIPS BETWEEN BED MATERIAL CHARACTERISTICS AND PARAMETERS FOR A UNIT CHANNEL

Bed Material Group	Bed Material Characteristics	Effective Hydraulic Conductivity K
		in/hr
1 Very high	Very clean gravel and large sand	>5
2 High loss rate	Clean sand and gravel, field conditions	2.0-5.0
3 Moderately high loss rate	Sand and gravel mixture with low silt-clay content	1.0-3.0
4 Moderate loss rate	Sand and gravel mixture with high silt-clay content	0.25-1.0
5 Insignificant to low loss rate	Consolidated bed material; high silt-clay content	0.001-0.10

the effective hydraulic conductivity of the stream channels to predict the transmission losses. A value of 2.0 inches per hour was used for streams in sectors II and VIII and 1.0 inch per hour in sector I (Table 6). These values represent average values for low to moderate silt and clay content. The calculated transmission losses will vary depending on the actual effective hydraulic conductivity selected.

Evapotranspiration

Consumptive use is the evaporation and transpiration from vegetation covered land areas (Wilson 1974, p. 41). Culler, Hanson and Jones (1976) estimated consumptive use of salt cedar and mesquite on a 25-mile reach of the Gila River over a nine-year study period using multi-temporal infrared aerial photography. Their monthly estimates of the consumptive use coefficient k and consumptive use factor f are shown in Figure 12a. They found the annual evapotranspiration ranged from 20 inches for 0% cover to 60 inches for 100% cover. The relationship between evapotranspiration and percent cover is linear above 50% cover and nonlinear below 50% cover (Figure 12b). Values of 48 and 36 inches for the 80-100% and 60-80% cover classes are probably more representative for the Sierrita site because of its higher elevation than the Gila River study area.

Water Balance

A water balance was calculated for each subsector based on the Walnut Gulch water balance proposed by Renard (1970, p. 22). Walnut Gulch is a 58-square-mile watershed near Tombstone, Arizona. Its climate and physiography are similar to the watersheds at the Sierrita

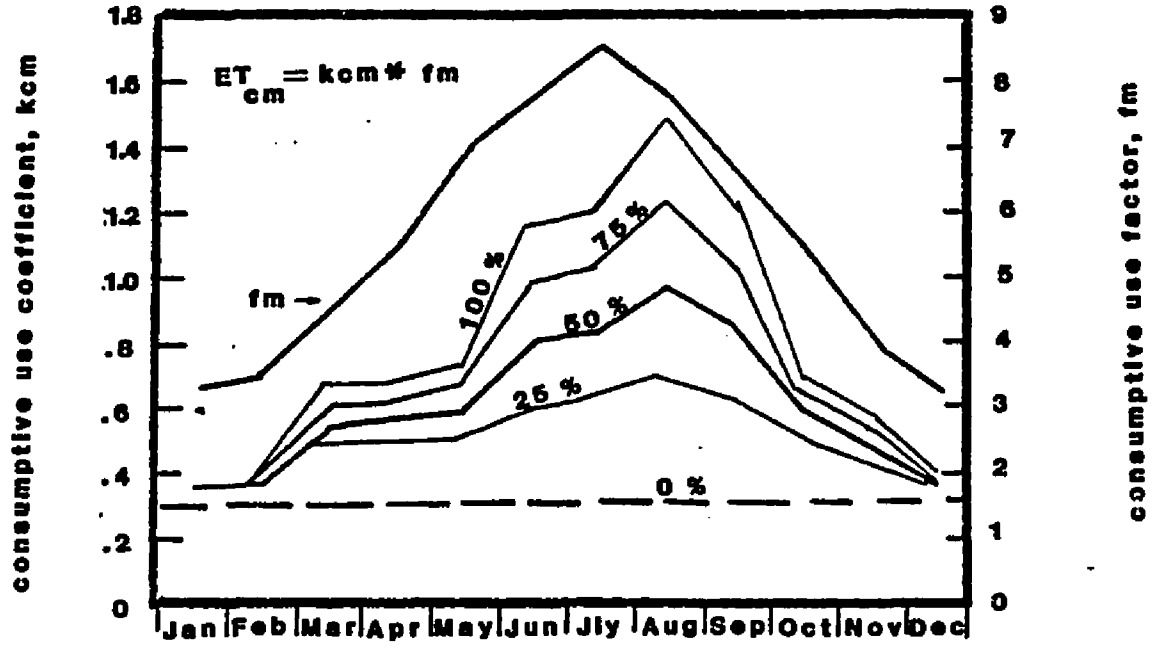

Figure 12a. Monthly Consumptive Use Coefficients kcm for Areas of Indicated Percent Phreatophyte Cover and Average Monthly Consumptive Use Factors fm (Culler, Hanson and Jones 1976).

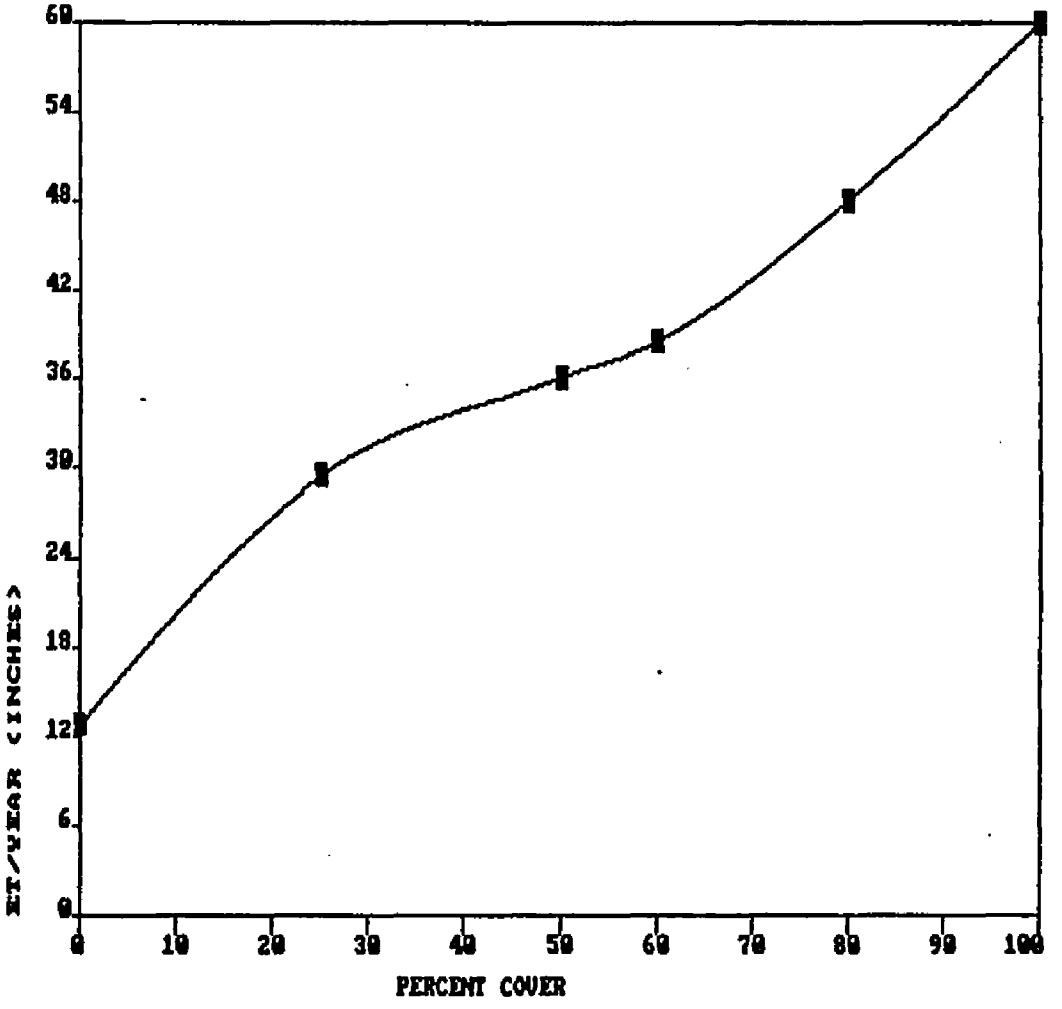

Figure 12b. Annual Evapotranspiration for Varying Percent - Phreatophyte Cover (Culler, Hanson and Jones 1976).

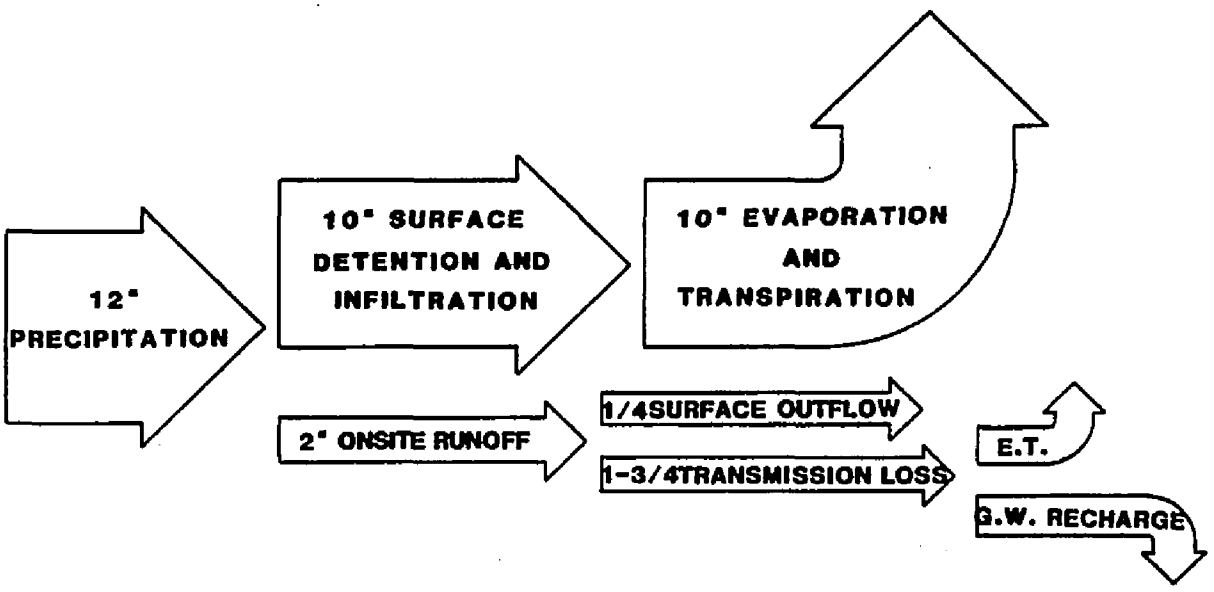

Figure 13. Water Balance of Walnut Gulch Watershed (Renard 1970)

TABLE 7

RESULTS OF WATER BALANCE CALCULATION

SECTOR		PRECIP. (in)	SURFACE DETENTION & INFILTRATION (acre ft.)	ET	RUNOFF (acre ft.)	SURFACE OUTFLOW (acre ft.)	TRANS. LOSS (acre ft.)
I	A	20	588	588	117	14	103
I	B	18	3326	3326	666	83	583
I	C	16	8266	8266	1657	207	1450
*I	D	14	15984	15984	3204	400	2804
I	E	12	33463	33463	6708	838	5870
I	F	10	43618	43618	8744	1093	7651
II	A	20	691	691	138	17	121
II	B	18	2482	2482	497	62	435
II	C	16	5063	5063	1015	126	888
II	D	14	7583	7583	1520	190	1330
*II	E	12	20557	20557	4121	515	3606
III	A	20	86	86	17	2	15
III	B	18	241	241	48	6	42
III	C	16	1625	1625	325	40	285
III	D	14	8037	8037	1611	201	1409
*III	E	12	8232	8232	1650	206	1444
IV	A	20	164	164	32	4	28
IV	B	18	404	404	81	10	70
IV	C	16	1016	1016	203	25	178
*IV	D	14	10790	10790	2163	270	1892
V	A	16	857	857	172	21	150
V	B	14	5041	5041	1010	126	884
*V	C	12	1727	1727	346	43	303
VI	A	20	310	310	62	7	54
VI	B	18	848	848	170	21	148
VI	C	16	3402	3402	682	85	596
VI	D	14	5016	5016	1005	125	880
VI	E	12	5000	5000	1002	125	877
*VI	F	10	5796	5796	1162	145	1016

TABLE 7--Continued

SECTOR	PRECIP. (in)	SURFACE DETENTION & INFILTRATION (acre ft.)	ET	RUNOFF (acre ft.)	SURFACE OUTFLOW (acre ft.)	TRANS. LOSS (acre ft.)
VII A	20	899	899	180	22	157
VII B	18	2116	2116	424	53	371
VII C	16	3424	3424	686	85	600
VII D	14	14784	14784	2964	370	2593
*VII E	12	6925	6925	1388	173	1214
VII F	10	11027	11027	2210	276	1934
VIIIA	20	414	414	83	10	72
VIIIB	18	1424	1424	285	35	249
VIIIC	16	2794	2794	560	70	490
*VIIID	14	5319	5319	1066	133	933
VIIIE	12	4222	4222	846	105	740
VIIIF	10	10366	10366	2078	259	1818
VIIIG	10	2286	2286	458	57	401

*Denotes subsectors that the SSC passes through.

site (Renard 1970, p. 1). Figure 13 shows how the precipitation is divided among losses and runoff. This distribution of precipitation was derived from field measurements at Walnut Gulch. The water balance for the Sierrita site was calculated using annual precipitation values. The results are listed in Table 7.

Results

The U.S. Soil Conservation Service runoff model and a water balance were applied at the Sierrita site to help explain the localized occurrence of a high-density riparian community on the southeast flank of the Sierrita Mountains. This area is believed to be partially underlain by a tuffaceous conglomerate. A red clay covers the interfluvial hills. The area receives 12 to 16 inches of precipitation annually. There are approximately 3.8 square miles of 80-100% vegetation cover and 5.6 square miles of 60-80% vegetation cover. The evapotranspiration of this vegetation is estimated at 48 and 36 inches per year for the 80-100% and 60-80% cover classes respectively.

The average annual precipitation values from MULT were approximately 16 inches for all subsectors. The precipitation values from Zauderer ranged from 10 to 20 inches. The discrepancy is due to the scope of the analyses used for each study. Henkel (1985) used 26 stations throughout Southeastern Arizona to predict the daily precipitation events at a given latitude, longitude and elevation. Zauderer considered eight stations in the immediate vicinity of the Sierrita site to produce an isohyetal map of the annual precipitation.

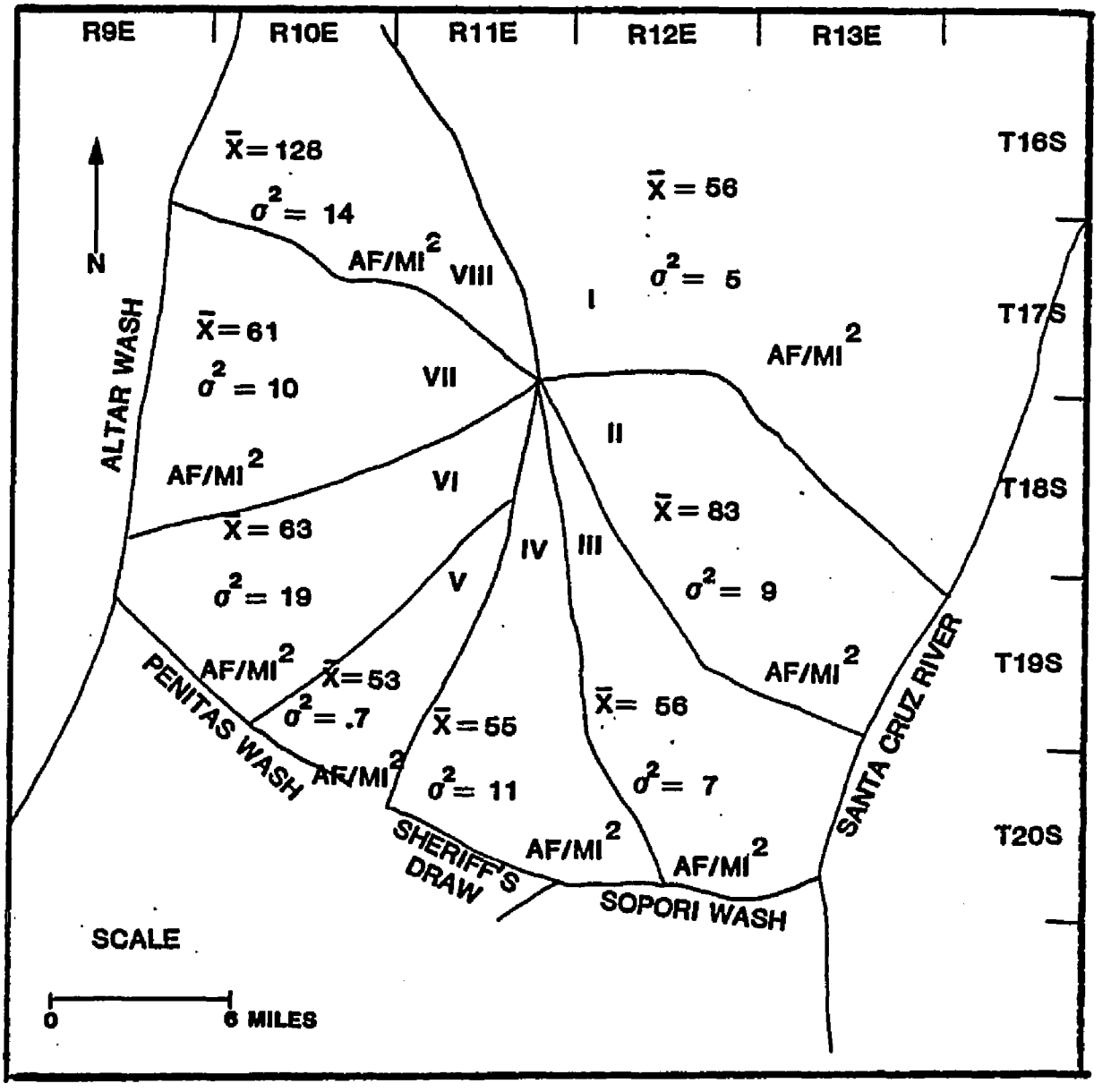

Figure 14. Mean and Variance of Surface Runoff Normalized to Sector Area

TABLE 8

WATER BALANCE FOR SECTORS AT THE SIERRITA SITE

SECTOR	SURFACE DETENTION & INFILTRATION (in)	ET (in)	RUNOFF (in)	SURFACE OUTFLOW (in)	TRANS. LOSS (in)
I	9.71	9.71	1.95	.24	1.71
II	11.04	11.04	2.21	.28	1.93
III	11.01	11.01	2.21	.28	1.93
IV	11.92	11.92	2.38	.30	2.08
V	11.38	11.38	2.29	.28	2.01
VI	10.41	10.41	2.08	.26	1.82
VII	10.48	10.48	2.10	.26	1.84
VIII	9.84	9.84	1.97	.24	1.72

The SCS model includes winter storms when calculating runoff. The water budget does not include winter storms because they generally do not generate much runoff. The runoff for sectors II and III as calculated by MULT were not significantly higher or lower than the other sectors at the site (Figure 14). The water budget for these sectors was very similar to the other sectors also (Table 8). The runoff and transmission losses calculated using the SCS runoff equation in MULT are not great enough to support the riparian vegetation with an evapotranspiration of 3 or 4 feet in sectors II and III. All of the other sectors can support the riparian vegetation therein. Analysis of the vegetation pattern in Figure 10 and field observations indicate the watersheds in sectors II and III consist of long, linear, narrow drainages separated by interfluvial hills covered with red clay and clayey loam, thus providing direct high surface runoff into the channels. The SCS model does not consider slope as a runoff factor and probably underestimates the amount of runoff in these sectors. The water balance calculations indicate the vegetation in sectors II and III can be supported if evaporation, transpiration and transmission loss water are included.

Renard (1970, p. 19) states that when the underlying geology is such that impervious layers beneath a channel limit the downward movement of water, recharge to the regional groundwater is low. Holding the transmission loss water in perched to local temporary aquifers increases the losses due to evaporation and transpiration. Vegetation that receives moisture from the temporary aquifers is generally found adjacent to the stream channels. The tuffaceous conglomerate that

underlies many of the drainages on the southeast flank may hold the runoff in a perched aquifer for use by the vegetation. This may explain the localized occurrence of the dense riparian vegetation on the southeast flank of the Sierrita Mountains.

CHAPTER 5

DELINEATION OF MOUNTAIN-PEDIMENT-BASIN BOUNDARIES

The presence of deep, clay-filled basins on the east side of the Maricopa Mountains affects the siting of the SSC. The areal extent of these basins needs to be determined so the impact on the SSC siting and construction can be evaluated.

The break in slope between mountains and pediments helps accurately map mountain ranges (Figure 15). The break in slope at the bottom of pediments does not necessarily mark the actual bottom of pediments or edges of basins. It is the bajada that abuts the pediment at this break in slope (Hastings 1986, p. 12). Groundwater running above the bedrock surface of the lower pediment may nourish deep-rooted vegetation over these areas. Thus, the edge of relatively unstressed vegetation near the pediment-bajada transition may denote the actual pediment-basin transition under favorable conditions (Hastings 1986, p. 14). Vegetation growing in lowland areas may signify a shallow water table near the edge of a basin or an area of relatively frequent surface runoff.

Mountain-Pediment Contacts

First approximations to the depth to bedrock can be made if the mountain-pediment and pediment-basin contacts can be located. The mountain-pediment contacts were located by a density slice of the

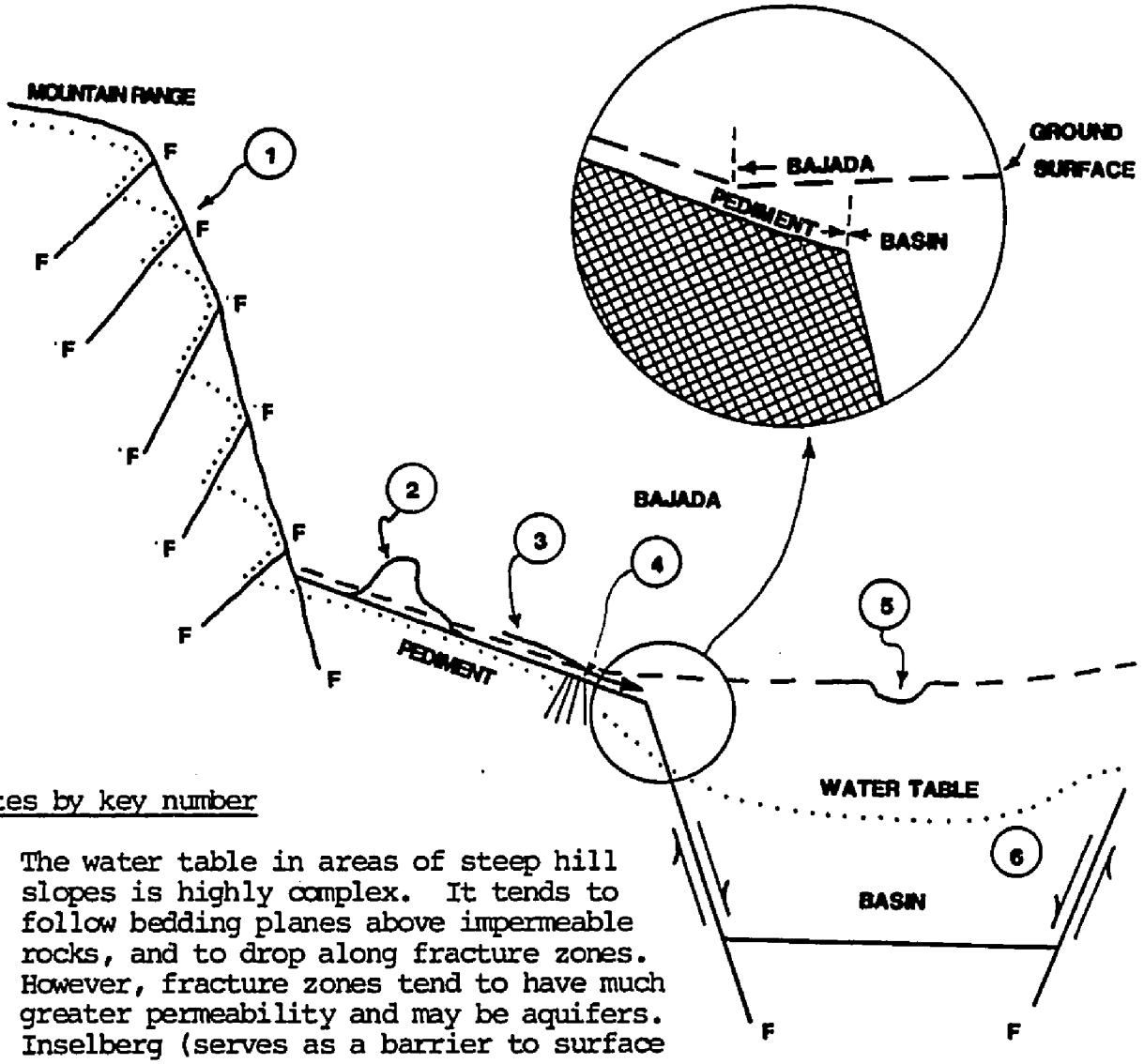

Notes by key number

1. The water table in areas of steep hill slopes is highly complex. It tends to follow bedding planes above impermeable rocks, and to drop along fracture zones. However, fracture zones tend to have much greater permeability and may be aquifers.
2. Inselberg (serves as a barrier to surface water flow).
3. Surface runoff (along the bedrock surface of the pediment).
4. Fractures in the pediment are a possible source of ground water.
5. Intermittent streams support riparian vegetation and may supply perched water tables that feed phreatophytes but which are unreliable as sources of ground water.
6. A basin contains deep aquifers in relatively porous media.

Figure 15. Effect of Landforms and Structure on Ground Water (Hastings 1986)

Maricopa Landsat MSS band 7 image. Bedrock outcrops have a lower reflectance in this band than the alluvium and vegetation and are easily separated from them.

Pediment-Bajada Contacts

The pediment-bajada contact was located based on the break in slope between the pediment and bajada. A slope magnitude image (Figure 16) was created from the Maricopa digital elevation data through the use of gradient filters. The data were first convolved with a 5 x 5 low-pass filter to smooth them. Then, Sobel filters were convolved in the x- and y- directions. The slope magnitude image was pseudocolored to make interpretation easier. The pediment-bajada boundary was interpreted as the break in slope between the solid tan area in Figure 16 and the tan contour lines. The tan contours are noise on the flat areas of the bajada and basins.

Basins

The Maricopa false-color composite in Figure 4 indicates a greater concentration of vegetation on the east side of the Maricopa Mountains. A MSS band 7/band 5 ratio was calculated to quantify the vegetation density (Figure 17). The color scheme described in Chapter 4 (page 26) was applied to this image. The densest vegetation occurs adjacent to the stream channels. Drainage density is inversely proportional to the infiltration capacity and transmissibility of the surface. Areas with low infiltration and transmissibility have higher drainage densities in order to efficiently carry off surface runoff. Higher drainage densities translate to greater vegetation density in

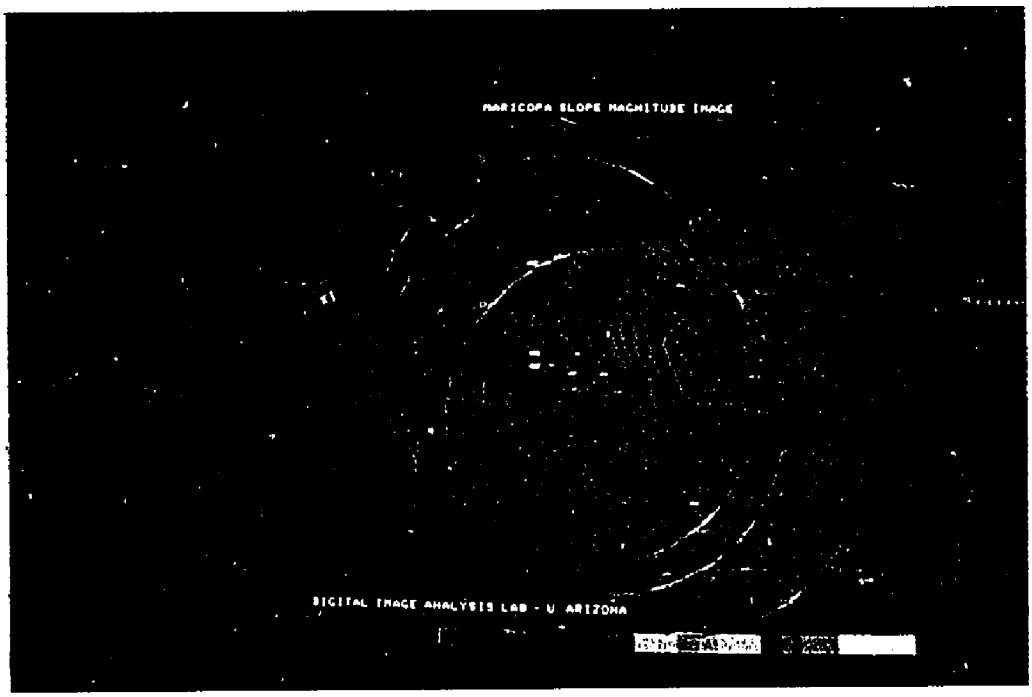

Figure 16. Slope Magnitude Image of Maricopa Digital Elevation Data

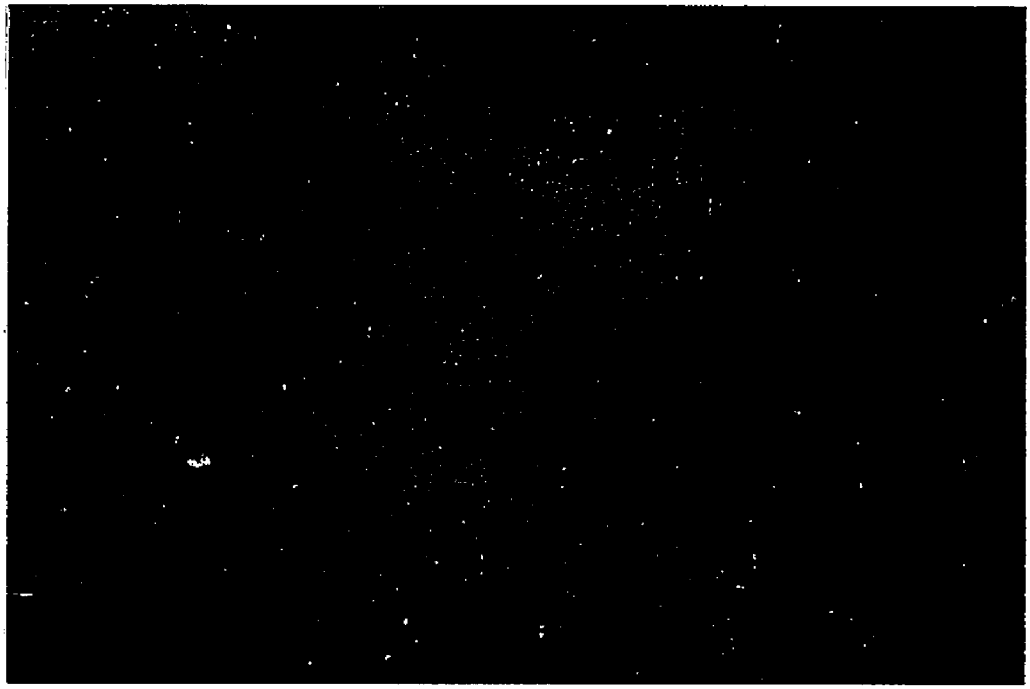

Figure 17. Vegetation Density for Maricopa Site

Figure 18. Bedrock Outcrop and Vegetation Density for Maricopa Site

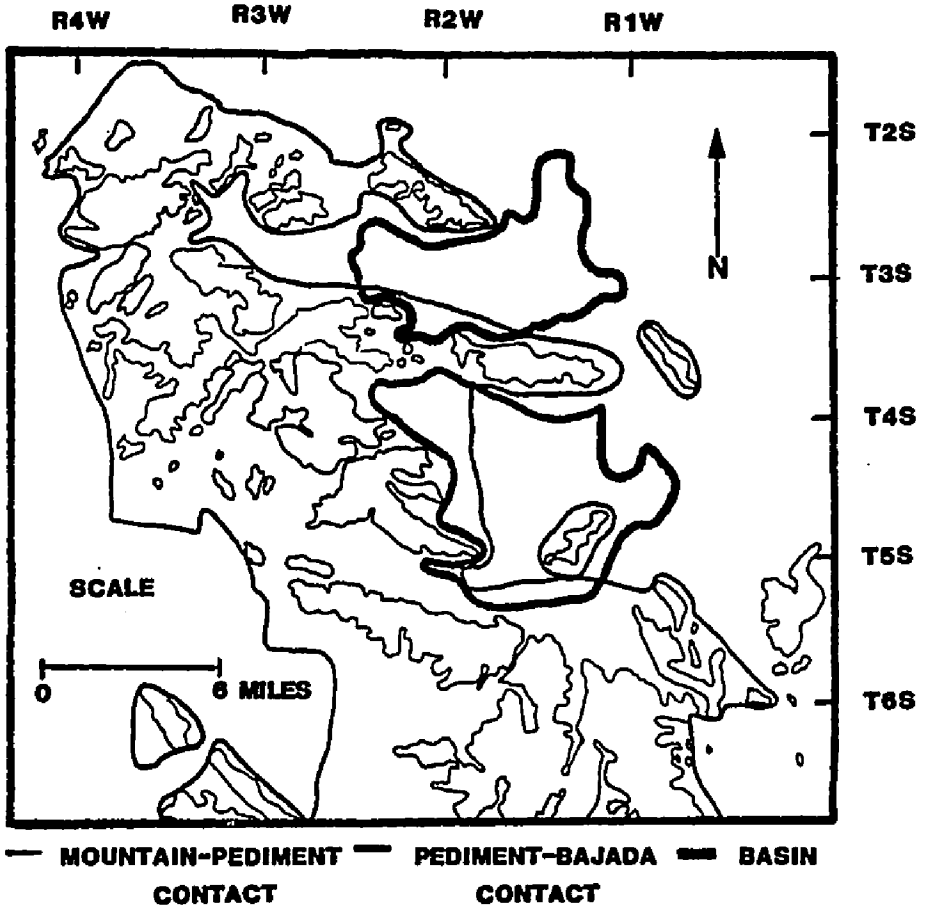

Figure 19. Mountain-Pediment-Basin Boundaries for Maricopa Site

arid areas. At the Maricopa site, the areas with high drainage densities overlie deep clay-filled basins. These basins can be mapped based on vegetation and drainage density. A density slice of the vegetation density was combined with the density slice of bedrock outcrop to show the location of the basins relative to the bedrock (Figure 18).

Results

Mountain-pediment-basin contacts were mapped by combining information from an MSS near-infrared band, slope magnitude image and vegetation density. These contacts are mapped in Figure 19. The southern basin mapped based on vegetation density extends further west than the pediment-bajada boundary. Vegetation growing in washes on the pediment may have been mistaken for vegetation growing in the basins. Or, the pediment-bajada boundary, as mapped from the slope magnitude image, may be extended too far eastward. The northern and southern basins as mapped from the vegetation density have an areal extent of 58 and 94 square kilometers respectively. The basins as mapped from a combination of the slope magnitude and vegetation density images have an areal extent of 55 and 58 square kilometers respectively.

CHAPTER 6

CONCLUSIONS

Analysis of vegetation density and distribution in digital images can aid in the interpretation of surface and subsurface geologic conditions. An MSS band 7/band 5 ratio image of the Sierrita site indicated a high density riparian community on the southeast flank of the Sierrita Mountains. Calculation of runoff, a water budget and evapotranspiration of the vegetation indicated that most of the Sierrita site had sufficient water available to support similar dense stands of vegetation. The fact that such dense riparian vegetation exists only on the southeast flank suggests some factor controlling the movement of the runoff rather than the amount. This factor may be an impermeable boundary retarding the deep infiltration of rainfall to the groundwater table. A tuffaceous conglomerate underlies portions of the southeastern portion of the Sierrita SSC site. This unit is very impermeable and may perch water in a temporary aquifer for use by the vegetation. The tuffaceous conglomerate weathers to a very gravelly, fine sandy loam that is found on the gently sloping low stream terraces in the southeastern portion of the site. The riparian vegetation grows in this soil unit. Subsurface geologic control is probably the most significant factor in the localized occurrence of the dense riparian vegetation on the southeast flank of the Sierrita Mountains.

An MSS band 7/band 5 ratio image of the Maricopa site indicated more vegetation on the east side of the Maricopa Mountains than the west side. The occurrence of this vegetation correlated with clay-filled basins. The clay forms an impervious surface which results in a higher drainage density. The runoff stays near surface and is available to support the vegetation. While the presence of clay may mean dense vegetation, the corollary is not necessarily true; dense vegetation does not always indicate the presence of clay. An attempt to more accurately map the basins was made by combining information from MSS band 5 and a slope magnitude image. This allowed the mountain-pediment-basin contacts to be mapped. The mapped pediment-bajada boundary may contain some error due to noise in the slope magnitude image. The relationship between vegetation density and basin location depends on the near-surface accumulation of relatively impermeable material. Alluvial-covered surfaces may not be detectable with this method and may cause some error in the mapping of the basins.

APPENDIX

CURVE NUMBERS AND AREAS FOR SUBSECTORS

Sector		Curve Number	Total Area Mi^2	Area Veg. (Mi^2) 80-100%	Area Veg. (Mi^2) 60-80%
I	A	83	.662	.642	.020
	B	83	4.16	.350	3.220
	C	83	11.63	---	1.304
	D	82	25.70	---	---
	E	82	62.77	---	---
	F	82	98.18	---	---
II	A	83	.778	.594	.184
	B	83	3.104	---	1.226
	C	90	7.123	---	.214
	D	90	12.192	.243	.477
	E	82	38.561	.740	2.452
III	A	83	.097	.039	.058
	B	83	.302	---	.253
	C	86	2.287	---	---
	D	82	12.922	.652	.846
	E	82	15.442	2.189	1.830
IV	A	83	.185	.107	.078
	B	83	.506	---	.117
	C	82	1.430	---	---
	D	82	17.349	.224	1.197
V	A	82	1.207	---	---
	B	82	8.105	---	---
	C	82	3.240	.399	---
VI	A	83	.350	.195	.155
	B	83	1.061	---	.438
	C	83	4.787	.632	.039
	D	82	8.066	.078	.253
	E	83	9.380	---	---
	F	83	13.048	---	---

CURVE NUMBERS AND AREAS FOR SUBSECTORS--Continued

Sector		Curve Number	Total Area Mi^2	Area Veg. (Mi^2) 80-100%	Area Veg. (Mi^2) 60-80%
VII	A	83	1.012	.778	.234
	B	83	2.647	.555	1.800
	C	83	4.817	---	2.024
	D	86	23.771	.068	.370
	E	78	12.990	---	---
	F	78	24.822	---	---
VIII	A	83	.467	.379	.088
	B	83	1.781	.107	1.674
	C	83	3.931	---	1.226
	D	86	8.553	---	---
	E	90	7.921	---	---
	F	90	23.333	---	---
	G	90	5.147	---	---

REFERENCES

Culler, R. C., R. L. Hanson and J. E. Jones. 1976. Relation of Consumptive use coefficient to the description of vegetation: Water Resources Research, Vol. 12, No. 1, pp. 40-46.

Curran, Paul. 1980. Multispectral remote sensing of vegetation amount: Progress in Physical Geography, Vol. 4, No. 3, pp. 315-342.

Davidson, E. S. 1973. Geohydrology and water resources of the Tucson Basin, Arizona: USGS Water Supply Paper 1939-E, 81 pp.

Davis, P. and S. Brooks. 1986. Report on hydrology of the Arizona Sierrita site SSC project: Univ. of Ariz. Dept. of Interdisc. Programs unpublished report, 19 pp.

Gates, D. M., H. J. Keegan, J. C. Schleter, V. R. Weidner. 1965. Spectral properties of plants: Applied Optics, vol. 4, no. 1, pp. 11-20.

Hastings, D. A. 1986. Combining Landsat and geophysical data for mineral and ground water exploration: An example from the Tucson area: publication in progress, 34 pp.

Henkel, Arthur F. 1985. Regionalization of Southeast Arizona precipitation distributions in a daily event-based watershed hydrologic model, Univ. of Ariz. unpublished master's thesis, 122 pp.

Kauth, R. J. and G. S. Thomas. 1976. The tasselled cap -- A graphic description of the spectral-temporal development of agricultural crops as seen in Landsat: Machine Processing of Remotely Sensed Data, pp. 41-51.

Knipling, Edward B. 1970. Physical and physiological basis for the reflectance and near-infrared radiation from vegetation: Remote Sensing of Environment, Vol. 1, pp. 155-159.

Krason, Jan, Antoni Wodzicki and Susan Cruver. 1982. Geology, energy and mineral resources assessment of Maricopa area, Arizona: Geoexplorers, Inc., unpublished report, 94 pp.

Lane, L. J. 1983. Transmission losses, Ch. 19. Nat. Eng. Handbook, Sec. 4, Hydrology, 21 pp.

_____. 1984. Surface water management: A user's guide to calculate a water balance using the CREAMS model: Los Alamos Nat. Lab., LA-10177M, 49 pp.

Perry, C. R., Jr., and L. F. Lautenschlager. 1984. Functional equivalence of spectral vegetation indices: Remote Sensing of the Environment, Vol. 14, pp. 169-182.

Ragan, R. M. and T. J. Jackson. 1975. Use of satellite data in urban hydrologic models: Jour. of the Hydraulics Div., ASCE, HY12, pp. 1469-1475.

Raines, G., T. Offield and E. Santos. 1978. Remote sensing and subsurface definition of facies and structure related to uranium deposits, Powder River Basin, Wyoming: Econ. Geol., Vol. 73, pp. 1706-1723.

Rango, A., J. Foster and V. V. Salomonson. 1975. Extraction and utilization of space acquired physiographic data for water resources development: Water Res. Bull., Vol. 11, No. 6, pp. 1245-1255.

Renard, K. G. 1970. The hydrology of semiarid rangeland watersheds: USDA ARS 41-162, 26 pp.

Rouse, J. W., Jr., R. H. Hass, J. A. Schell and D. W. Deering. 1973. Monitoring vegetation systems in the great plains with ERTS: Proc. Third ERTS Symposium, NASA SP-351, Dec. 1973, Vol. I, pp. 309-317.

Rowan, Lawrence C. and Ernest H. Lathram. 1980. Mineral exploration, in Remote Sensing in Geology, pp. 553-605. Eds. Barry S. Siegal and Alan R. Gillespie. New York: John Wiley and Sons, 702 pp.

SSC Central Design Group. 1985. Superconducting Super Collider siting parameters document: Unpublished report, Lawrence Berkeley Laboratory, Univ. of Calif., 48 pp.

Tucker, C. J. 1978. A comparison of satellite sensor bands for vegetation monitoring: Photogrammetric Eng. and Remote Sensing, Vol. 44, No. 11, pp. 1369-1380.

Universities Research Association. 1985. To the Heart of Matter - The Superconducting Super Collider, 36 pp.

USCS. 1972. Hydrology Nat. Eng. Handbook, Sec. 4.

Wilson, E. M. 1974. Engineering Hydrology. London: Macmillan Press Ltd., 232 pp.

Zauderer, J. 1986a. Sierrita site climate: Univ. of Ariz. Dept. of Interdisc. Programs unpublished report, 26 pp.

_____. 1986b. Soils at the SSC circumference: Univ. of Ariz. Dept. of Interdisc. Programs unpublished report, 52 pp.